Multiband negative refraction in one-dimensional photonic crystals

J.E. Lugo[1], B. de la Mora[1,2], R. Doti[1], R. Nava[2], J. Tagueña[2], A. del Rio[2] and J.Faubert[1*]

[1]Visual Psychophysics and Perception Laboratory, School of Optometry, University of Montreal, C.P. 6128 succ. Centre Ville, Montreal, Quebec, Canada H3C3J7. http://vision.opto.umontreal.ca
[2]Centro de Investigación en Energía, Universidad Nacional Autónoma de México, Temixco 62580, Morelos, Mexico
**Corresponding author: jocelyn.faubert@umontreal.ca*

Abstract: We simulate a lossless one-dimensional photonic crystals (1D-PC) structure and show that negative refraction could be present near the low frequency edge of at least the second, fourth and sixth bandgaps. We experimentally demonstrate for the first time negative refraction in strongly modulated porous silicon 1D-PC in the visible and near infrared regions. This 1D-PC structure may allow the realization of short-focus Veselago lenses in different optical bands. An advantage of our structure is its simplicity allowing for cheap and rapid fabrication of samples.

OCIS codes:(260.2110) Electromagnetic optics; (080.3630) Lenses; (120.2440) Filters; (160.4236) Nanomaterials; (160.5298) Photonic crystals.

References and links

1. V. G. Veselago, "The electrodynamics of substances with simultaneously negative values of permittivity and permeability," Sov. Phys. USPEKHI **10**, 509 (1968).
2. J. B. Pendry, "Negative refraction makes a perfect lens," Phys. Rev. Lett. **85**, 3966-3999 (2000).
3. D. F. Sievenpiper, M. E. Sickmiller, and E. Yablonovitch, "3D wire mesh photonic crystals," Phys. Rev. Lett. **76**, 2480-2483 (1996).
4. A. V. Kavokin, G. Malpuech, and I. Shelykh, "Negative refraction of light in Bragg mirrors made of porous silicon," Phys. Lett. A **339**, 387–392 (2005).
5. V. M. Agranovich, Y. R. Shen, R. H. Baughman, and A. A. Zakhidov,"Linear and non linear wave propagation in negative refraction metamaterials," Phys. Rev. B **69**, 165112 (2004).
6. P. V. Parimi, W. T. Lu, P. Vodo, J. Sokolo, J. S. Derov, and S. Sridhar, "Negative refraction in 1D photonic crystals," Phys. Rev. Lett. **92**, 127401 (2004).
7. H. Kosaka, T. Kawashima, A. Tomita, M. Notomi, T. Tamamura, T. Sato, and S. Kawakami, "Superprism phenomena in photonic crystals," Phys. Rev. B **58**, R10096 (1998).
8. E. Cubukcu, K. Aydin, E. Ozbay, and S. Soukoulis, "Subwavelength Resolution in a Two-Dimensional Photonic-Crystal-Based Superlens," Phys. Rev. Lett. **91**, 207401 (2003).
9. C. Luo, S. G. Johnson, J. D. Joannopoulos, and J. B. Pendry,"Subwavelength imaging in photonic crystals," Phys. Rev. B. **68**, 045115 (2003).
10. H. Kosaka, T. Kawashima, A. Tomita, M. Notomi, T. Tamura, T. Sato, and S. Kawakami, "Self-collimating phenomensa in photonic crystal," Appl. Phys. Lett. **74**, 1212 (1999).
11. E. Cubukcu, K. Aydin, E. Ozbay, S. Foteinopoulou, and C. M. Soukoulis, "Negative refraction by photonic crystals," Nature **423**, 604 (2003).
12. P. V. Parimi, W. T. Lu, P. Vodo, and S. Sridhar, "Photonic crystals: Imaging by flat lens using negative refraction," Nature **426**, 404 (2003).
13. A. Berrier, M. Mulot, M. Swillo, M. Qiu, L. Thylén, A. Talneau, and S. Anand, "Negative Refraction at Infrared Wavelengths in a Two-Dimensional Photonic Crystal," Phys. Rev. Lett. **93**, 073902 (2004).
14. E. Schonbrun, Q. Wu, W. Park, T. Yamashita, C. J. Summers, M. Abashin, and Y. Fainman, "Wave front evolution of negatively refracted waves in a photonic crystal," Appl. Phys. Lett. **90**, 041113 (2007).
15. R. Moussa, S. Foteinopoulou, L. Zhang, G. Tuttle, K. Guven, E. Ozbay, and C. M. Soukoulis, "Negative refraction and superlens behavior in a two-dimensional photonic crystal, " Phys. Rev. B **71** 085106 (2005).
16. C. Luo, S. G. Johnson, J. D. Joannopoulos, and J. B. Pendry, "Negative refraction without negative index in metallic photonic crystals," Opt. Express **11**, 746 (2003).
17. S. Foteinopoulou and C. M. Soukoulis, "Electromagnetic wave propagation in two-dimensional photonic crystals: A study of anomalous refractive effects," Phys.Rev. B **72,** 165112 (2005).

#105441 - $15.00 USD Received 18 Dec 2008; revised 7 Feb 2009; accepted 9 Feb 2009; published 13 Feb 2009

18. C. Yuan Yuan, H. Z. Ming, S. J. Long, L. C. Fang, and Q. Wang, "Frequency bands of negative refraction in finite one-dimensional photonic crystals," Chin. Phys. **16**, 173 (2007).
19. P. Vodo, P. V. Parimi, W. T. Lu, S. Sridhar, and R. Wing, "Microwave photonic crystal with tailor made negative refractive index," Appl. Phys. Lett. **85**, 1858 (2004).
20. Z. Feng, X. Zhang, Y. Wang, Z. Y. Li, B. Cheng, and D. Z. Zhang, "Negative Refraction and Imaging Using 12-fold-Symmetry Quasicrystals," Phys. Rev. Lett. **94**, 247402 (2005).
21. M. Notomi, "Negative refraction in photonic crystals," Opt. Quantum Electron. **34**, 133 (2002).
22. G. Boedecker and C. Henkel, "All-frequency effective medium theory of a photonic crystal," Opt. Express **11**, 1590 (2003).
23. R. Srivastava, B. K. Thapa, S. Pati, and S.P. Ojha, "Negative refraction in 1D photonic crystals," Solid State Commun. **147**, 157–160 (2008).
24. J. Yao, Z. Liu, Y. Liu,Y. Wang, C. Sun, G. Bartal, A. M. Stacy, and X. Zhang, "Optical Negative Refraction in Bulk Metamaterials of Nanowires," Science **321**, 930 (2008).
25. R. Nava, M. B. de la Mora, J. Tagüeña-Martínez, and J. A. del Río, "Refractive index contrast in porous silicon multilayers," Phys. Status Solidi A (To be published).
26. L. Pavesi,"Porous silicon dielectric multilayers and microcavities," La Rivista del Nuovo Cimento **20**, 1 (1997).
27. W. Q. Zhang and F. Yang, "Negative refraction at various crystal interfaces," Opt. Commun. **281**, 3081-3086 (2008).
28. S. Foteinopoulou, E. N. Economou, and C. M. Soukoulis, "Refraction in Media with a Negative Refractive Index," Phys. Rev. Lett. **90**, 107402 (2003).

1. Introduction

Negative refraction of light is widely discussed now as a tool to achieve short focus Veselago lenses [1]. These lenses have been realized in the microwave region [2,3], but visible light remains an unsolved problem up to now. There are present discussions as to how veselago lenses could be achieved for visible light. A few natural candidates for achieving this include metamaterials, plasmonic modes and photonic crystals [4]. Metamaterials are materials composed of metal/dielectric composites that present negative refraction in the far-field regime [5]. However, the absorption loss in the metal limits potential optical applications. Photonic crystals (PC) are artificial structures that show an extraordinary strong nonlinear dispersion at wavelengths close to the bandgap. Under certain conditions, they abnormally refract the light as if they had a negative refractive index [6-9]. A PC can even focus diverging light owing to the negative refraction at the flat boundary [10]. Negative refraction has been observed in two-dimensional PC (2D-PC) into the microwave and infrared region [6,11-15]. Extensive numerical [9,16-18] and experimental studies [19-21] have provided a better understanding of negative refraction in photonic crystals. For instance, when light propagation in strongly modulated, 2D-PC becomes refraction-like in the vicinity of the photonic bandgap. Such a crystal behaves like a material having an effective refractive index controllable by the band structure. Boedecker and Henkel [22] found that the simple one-dimensional (1D) Kronig–Penney model provided an exactly soluble example of a photonic crystal with negative refraction. Recently it has been theoretically shown that negative refraction in 1D-PC may occur near the low frequency edge of the second and fourth bandgaps [18,23]. Moreover creating photonic crystals that exhibit negative refraction for visible light remains a major challenge because of fabrication difficulties and, up to today, negative refraction at visible wavelengths has been shown only in bulk metamaterials of nanowires [24]. Here, we demonstrate negative refraction in strongly modulated porous silicon (Psi) 1D-PC in the visible and near infrared regions that may allow the realization of short-focus Veselago lenses as the ones discussed in [4], where a structure made of two 1D-PC with one rotated by 90◦ with respect to the other is proposed. An advantage of Psi based structures is that this material allows for the rapid growth of thick multilayer structures with a high contrast of the refractive indices governed by the degree of porosity.

#105441 - $15.00 USD Received 18 Dec 2008; revised 7 Feb 2009; accepted 9 Feb 2009; published 13 Feb 2009

2. Sample fabrication and characterization

Psi multilayers (Fig. 1 (a)) were prepared by electrochemical anodization of crystalline silicon [25]. Porous silicon was fabricated by wet electrochemical etching of highly boron-doped c-Si substrates with orientation (100) and electrical resistivity of 0.001-0.005 Ω-cm (room temperature= 25 ° C, humidity= 30%). On one side of the c-Si wafer, an aluminium film was deposited and then heated at 550ºC during 15 minutes in nitrogen atmosphere to produce a good electrical contact. In order to have flat interfaces, an aqueous electrolyte composed of HF/ethanol/glycerol was used to anodize the silicon substrate. It is well known that the Psi refractive index increases by decreasing the electrical current applied during the electrochemical etching. However, reducing the porosity too much might stop the electrolyte flow through the porous and limit the subsequent high porosity layer that makes the contrast. One way to allow the electrolyte to flow is by increasing the ethanol fraction in the solution. For this reason, an electrolyte composition of 3:7:1 was used. In addition, the HF concentration was maintained constant during the etching process using a peristaltic pump to circulate the electrolyte within the Teflon™ cell. Anodization begins when a constant current is applied between the c-Si wafer and the electrolyte by means of an electronic circuit controlling the anodization process. To produce the multilayers, current density applied during the electrochemical dissolution was alternated from 3 mA/cm^2 (layer a) to 40 mA/cm^2 (layer b) and eighty periods (160 layers) were made. Psi samples were partially oxidized at 350 °C for 10 min. oxidation induces a blueshift in the peak reflectivity due to the decrease in the refractive indices of the layers, but it is necessary to stabilize the samples.

The reflectivity was measured to know the photonic band gap structure in the y-direction (Fig. 1(b)). Reflectivity spectra of the samples were taken with a Shimadzu UV1601 ultraviolet–visible spectrophotometer at 5° incidence and scanning electron microscopy (SEM) was used to measure the films thicknesses which were 326±11 nm (a) and 435 ±11 nm (b). The theoretical photonic bandgaps locations were obtained from the band edge condition given by the following equation:

$$\cos\left(\frac{\omega n_a a}{c}\right)\cos\left(\frac{\omega n_b}{c}\right)-\frac{1}{2}\left(\frac{n_a}{n_b}+\frac{n_b}{n_a}\right)\sin\left(\frac{\omega n_a a}{c}\right)\sin\left(\frac{\omega n_b}{c}\right)=\pm 1.$$

Where ω is the light frequency and c is the light speed. The best refractive index values we found that fit the experimental photonic bandgap structure are $n_a = 1.1$ and $n_b = 2$ (Fig.1(c), green bands). We have experimentally measured the refractive indexes of single Psi layers made with the same electrochemical conditions as for the multilayers [25] and we found that $n_a = 1.4$ and $n_b = 2.2$. Nevertheless, it is known that the refractive index and etching rate for a single layer are modified in the presence of a multilayer structure up to approximately 14%, a phenomenon that has been systematically observed [26]. This result might have the consequence of compromising the mechanical stability of the structure. Indeed, in certain regions seen in Fig. 1(a) layers appear to be collapsed. Nevertheless Fig. 1(b) clearly shows that a photonic bandgap structure in our samples is maintained. Negative refraction was observed in all our experiments where several regions were scanned .

#105441 - $15.00 USD Received 18 Dec 2008; revised 7 Feb 2009; accepted 9 Feb 2009; published 13 Feb 2009

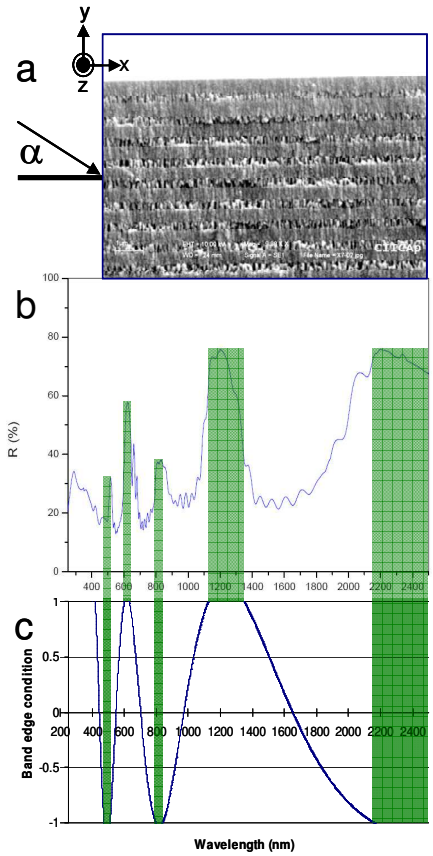

Fig. 1. 1D-PC characteristics (a) SEM picture of Psi structure. (b) The reflectivity spectrum. (c) Photonic band structure calculated from the band edge condition (green bands).

3. Negative refraction condition

In references [18] and [23] the negative refraction in 1D-PC is theoretically studied by using the transfer matrix method and Bloch theorem. In these works, the photonic band structure and group velocity is studied, and with the help of group velocity and power transmittance, they have obtained the frequency bands of negative refraction and found that negative refraction may occur near the low frequency edge of the second, fourth and even the sixth bandgaps where the group velocity component that is parallel to the layers is negative (V_{gll}). They conclude that if light falls obliquely on the y-direction interface (Fig. 1(a)) then when $V_{gll} > 0$, the wave refracts according to the classical Snell law; $V_{gll} = 0$ is associated with the perpendicular propagation; but $V_{gll} < 0$ means the transmitting beam will bend to the 'wrong' side, that is the same side as the incident beam resulting in negative refraction if the beam passes through the 1D-PC. Here, light impinges obliquely on the *x*-direction interface with an incidence angle α (Fig.1(a)), so we expect that to obtain negative refraction we need to look where the group velocity component that is perpendicular to the layers is negative ($V_{g\perp}$). In other words, the negative refraction condition in this example is obtained by the fact that if light impinges obliquely with frequency values near the low frequency edge of the second, fourth and sixth bandgap (Fig. 2(a)) the group velocity component that is perpendicular to the layers is negative (Fig. 2(b)) and consequently the effective mass is negative in the same region (Fig. 2(c)). Note that we are not claiming that a negative effective mass implies the

#105441 - $15.00 USD Received 18 Dec 2008; revised 7 Feb 2009; accepted 9 Feb 2009; published 13 Feb 2009

negative refraction but under the aforementioned conditions it is true that negative effective mass implies negative refraction. However a simple contradiction for that is when the structure is excited with larger tangential wavevectors. In such cases, it can be seen that both positive and negative refraction are possible for a region with negative effective mass [27]. Indeed in Fig. 2 we can observe that, near the high frequency edge of the first bandgap, the effective mass is negative but the group velocity is positive. The results in Fig. 2 were obtained by a similar calculation for the band edge condition, perpendicular group velocity and effective mass as in references [4,18,23] for an angle of 25 degree. The effective mass calculation is a second order approximation of the frequency dispersion relation in Taylor's series and it is only valid for frequencies close to the band edges. Now that we have clarified this point, in the following we will analyze more in detail the effective mass approximation in our structure. The medium we consider is strongly anisotropic (Fig. 1(a)), so that the effective masses have different signs in (x,z)-plane and y-direction. For instance, the second (1345 nm-1680 nm) and fourth (630 nm-711 nm) allowed bands (Fig. 3, yellow lines) are characterized by a negative parabolicity in the y-direction. The (x,z)-plane dispersion is also parabolic close to the band edge but is characterized by a positive effective mass (not shown) similar to the one reported in [4]. The negative parabolicity interval was calculated by taking the second derivative of the second and fourth dispersion bands. Therefore we fitted a parabola in the interval where the second derivative was negative. The two fitted polynomials are shown in Fig. 3 with their correspondent correlation coefficients. The polynomials $\alpha(ka/\pi)^2+\beta(ka/\pi)+\gamma$ can be rewritten as $\alpha^*(ka/\pi)^2+\gamma$ where $\alpha^*=\alpha[1+(\beta/\alpha k)]$. The effective mass approximation is obtained for small (ka/π), which is equivalent to the condition $|\alpha^*|\rangle\rangle|\alpha|$. For light with wavelengths of 1350 nm and 633 nm we obtained α^* values of -5.35 and -8.68 respectively. Since the band structure in the y-direction for TE or TM polarization are the same the effective mass approximation is also the same for both polarizations. It is clear that given the periodicity of the band structure in the y-direction we would find the next negative refraction region lying in the sixth allowed band between 418 nm and 446 nm (Fig. 2 shows approximately the three negative refraction regions as yellow bands). The dispersion of photonic modes and the photonic bandgaps in an infinite periodic structure shown in Fig. 3 were calculated by using the well known transfer matrix techniques.

#105441 - $15.00 USD Received 18 Dec 2008; revised 7 Feb 2009; accepted 9 Feb 2009; published 13 Feb 2009

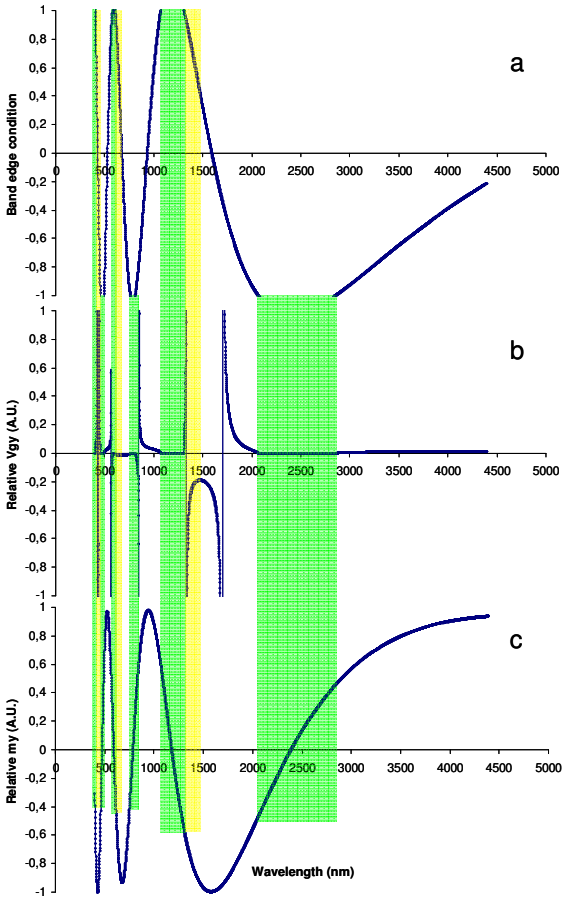

Fig. 2. 1D-PC negative refraction condition properties (a) Band edge condition. (b) Relative perpendicular group velocity. (c) Relative effective mass. The green bands show the band edges and the yellow bands show approximately the three negative refraction bands inferred from the negative parabolicity of the y-direction bands . The angle of incidence is 25 degrees with TE polarization.

#105441 - $15.00 USD Received 18 Dec 2008; revised 7 Feb 2009; accepted 9 Feb 2009; published 13 Feb 2009

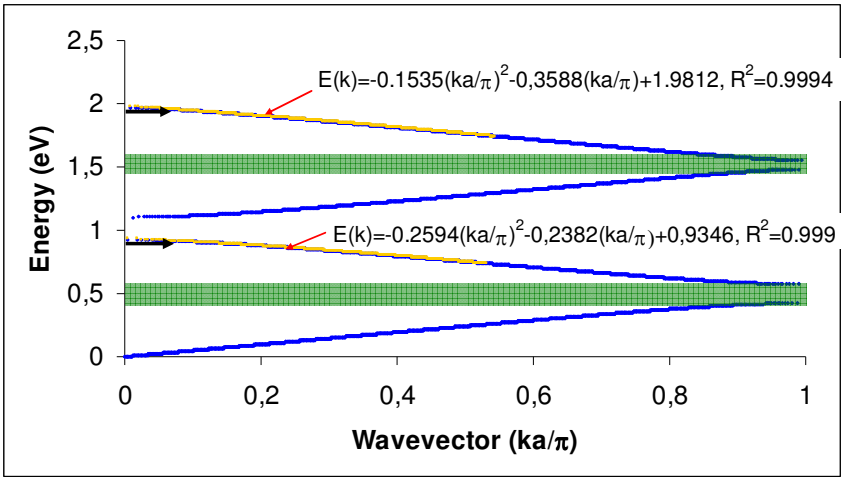

Fig. 3. Schematic illustration of the negative refraction condition in the band structure. The parameter **a** represents the multilayer period. The black arrows show the energy of the wavelengths we used experimentally.

4. Finite element simulations

We performed full-wave simulations for TE and TM polarization light (by FEMLAB 3.1) considering the experimental thickness we found and refractive indices we inferred from the band structure fitting (optical losses were neglected) and we simulated 80 periods. The incidence angle was varied until there was a clearly observed negative refraction in three different bands. Finite element simulations at 419 nm, 633 nm and 1350 nm confirm the theoretical predictions (Fig. 4). Monochromatic TE and TM polarized plane waves impinge at an angle of 25 degrees from air to the multilayers in the (x,y)-plane. One can see that, at the boundary, the plane waves are negatively refracted where the power itself changes its propagation direction showing a pronounced negative refraction and it is concentrated close to the interface (Fig. 4 top, power outflow distributions). These images are very similar to ones obtained for a 2D-PC [28]. It is clear from Fig. 4 that in all the cases we simulated there is an amount of power that propagates normally to the interface inside the 1D-PC (this is more evident in the 1350 nm case). Since the three wavelengths we used are outside the bandgap regions, $V_{g\perp} = 0$ and $V_{gll} \neq 0$ it is normal to have power propagating in that direction. In a perfect 1D-PC the Bloch waves are evanescent in the bandgap and they decay to zero. However in a finite 1D-PC we should expect power transmissions even inside the bandgap. Figure 5 shows the propagation of three wavelengths with incidence angle $\alpha = 0$. It is clear that the transmitted power decreases from the first negative refraction band (1350 nm) to the third one (419 nm). These results agree well with the ones presented in [18,23]. Moreover, in the 419 nm case, the incident region appears to be significantly different. This might be due to wavelength scattering in the x-direction interface because 419 nm is less than the structure period of 761 nm. Indeed the same phenomenon is noticeable for the x-direction interface at 633 nm.

#105441 - $15.00 USD Received 18 Dec 2008; revised 7 Feb 2009; accepted 9 Feb 2009; published 13 Feb 2009

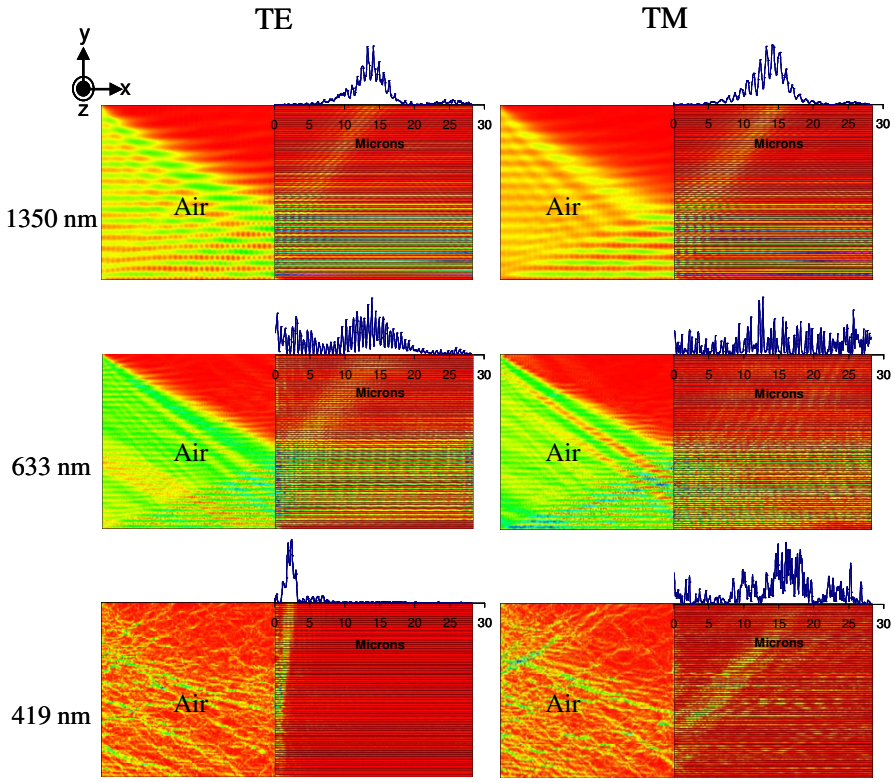

Fig. 4. Finite element simulations at 419 nm, 633nm and 1350nm with monochromatic TE and TM polarized plane waves at an angle of 25 degrees. The blue graphs on top of each simulation represent power outflow distributions.

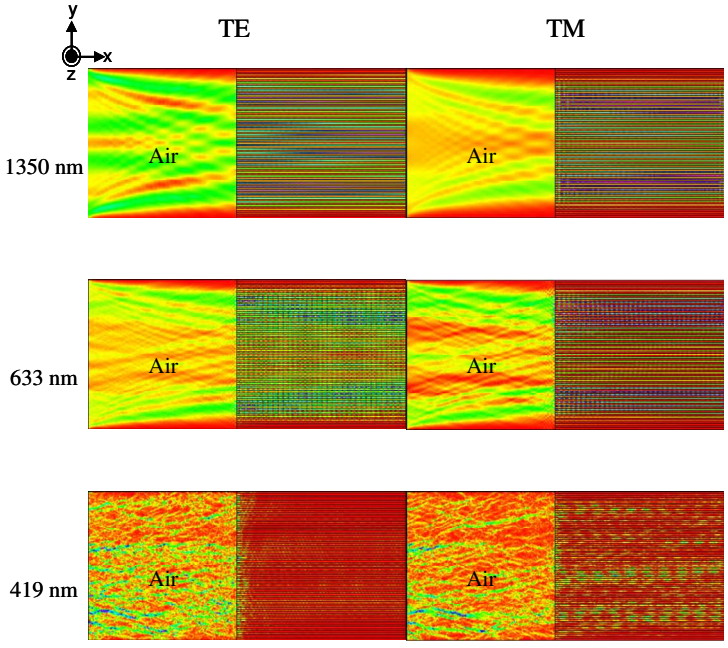

Fig. 5. Finite element simulations at 419 nm, 633nm and 1350nm with monochromatic TE and TM polarized plane waves at an angle of 0 degrees.

#105441 - $15.00 USD Received 18 Dec 2008; revised 7 Feb 2009; accepted 9 Feb 2009; published 13 Feb 2009

5. Experimental results

From Fig. 1(a) it is clear that the experimental photonic bandgap structure is smeared out below 500 nm and experimentally we cannot expect any negative refraction there. For this reason we used only 633 nm and 1350 nm wavelengths to investigated negative refraction. Figure 6 shows our experimental setup. The sample (Component 6) with the pinhole (Component 4) (NT39-730, Edmund Optics) was illuminated by a broad band source (Component 1) (Optronic Laboratories, 740-20A, tungsten lamp 300W) and to obtain the desired monochromatic light we have used two band-pass filters (Component 3) (633FS10-12.5 and 135FS10-12.5, Andover Corporation) at 633 nm and 1350 nm (both have a 10 nm bandwidth). The TE or TM polarization was selected by using two linear polarizers (Component 2) (NT 48-545 and NT48-887, Edmund Optics), and the negative refractive transmitted light was captured by two CCD cameras (KP-D50, Hitachi) and (Micron-viewer 7290A, Electrophysics) coupled with a singlet lens (Component 9) (focal length of 8 mm, NT-45114, Edmund Optics) placed at 8 mm from the sample. The sample and the camera were mounted on linear and rotary mechanical stages. The XYZ linear stages (Daedal Inc) had a resolution of 1 micron and the rotary stages (MR150, Aerotech) had a resolution of 2.5 arc minutes. The TE or TM Polarized monochromatic light beam (Component 5) illuminated the sample at an angle of 25 degrees through a 1 mm pinhole placed at 3 mm from the sample. The beam was focused in the x-direction interface in a way that light never hit the y-direction interface. This was performed very carefully by scanning the focused light beam from the crystalline silicon substrate towards the y-direction interface. The cameras were centered at 25 degrees (angle β) but their positions were compensated to account for the positive refraction that the negative refraction beam (Component 7) suffers at the exit of the y-direction interface. This was done by using Snell's law and an effective refractive index value of 1.6 for the multilayer structure. Once everything was in place we scanned the sample on the z-direction (see component 9) and when a spot image was captured we measured the distance from the x-direction interface to the image (Δx was corrected due to the sample rotation) by using the micrometer screw of the linear stage. This was possible because our imaging system was capable to give us enough resolution to mark on a screen the x-direction interface and the spot image. The components 9a-9d show four images corresponding to 1350 nm and 633 nm (TE and TM polarizations). The spots are located at a distance of approximately $\Delta x = 16$ microns from the interface (x-direction) which agreed with our numerical simulations.

6. Conclusions

In conclusion, we have shown that a simple 1D-PC can present negative refraction in multiple bands. Experimentally we have demonstrated that a 1D-PC based on the nanostructure porous silicon can exhibit negative refraction simultaneously in infrared and visible light regions and may allow the realization of short-focus Veselago lenses as the ones discussed in [4], where a structure made of two 1D-PC with one rotated by 90◦ with respect to the other is proposed. An advantage of Psi based structures is its simplicity allowing for cheap and rapid fabrication of samples. Finally, in order to gain more insight on the negative refraction phenomenon in 1D-PCs more detailed experiments are needed. For instance, angle dependent measurements and monitoring the response as a function of wavelength. We are currently performing experimental work in this direction.

#105441 - $15.00 USD Received 18 Dec 2008; revised 7 Feb 2009; accepted 9 Feb 2009; published 13 Feb 2009

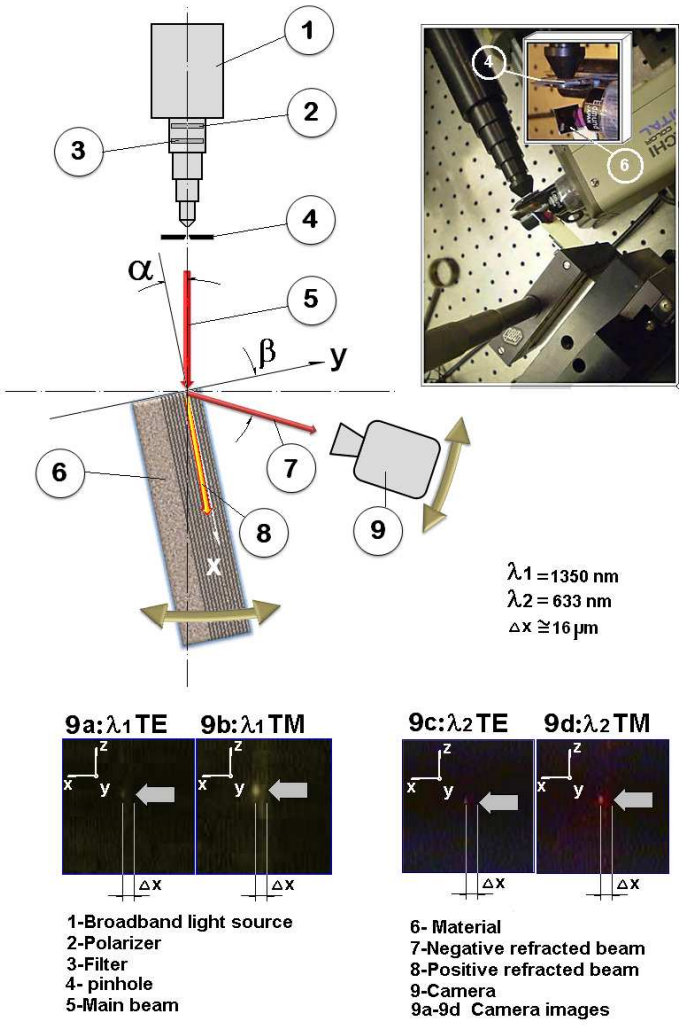

Fig. 6. A cartoon of the experimental setup (with the nine components) for the negative refraction observation and a picture of the real experimental setup. Both the sample and the camera are placed in translational and rotational stages. A broadband source along with bandpass filters and linear polarizers were used to explore the infrared and visible negative refraction bands. Captured images for the different conditions are shown in 9a-9d.

Acknowledgments

This work was supported by the NSERC-Essilor Research Chair and an NSERC operating grant and by DGAPA IN103608 grant. The authors thank Gildardo Casarrubias and Rene Guardian for the sputtering system and SEM pictures, Dr.Shiwei Huang and Patrick Perron for technical assistance, the photonic systems group at McGill University for providing the infrared camera and software simulations. B. de la Mora thanks CONACyT for providing financial support for a visitor's fellowship at University of Montreal.

#105441 - $15.00 USD Received 18 Dec 2008; revised 7 Feb 2009; accepted 9 Feb 2009; published 13 Feb 2009